AMERICAN SOCIETY FOR MICROBIOLOGY | Journal of Bacteriology®

RESEARCH ARTICLE

Functioning of Mycobacterial Heat Shock Repressors Requires the Master Virulence Regulator PhoP

Ritesh Rajesh Sevalkar,[a]* Divya Arora,[b] Prabhat Ranjan Singh,[a] Ranjeet Singh,[a]* Vinay K. Nandicoori,[b] Subramanian Karthikeyan,[a] Dibyendu Sarkar[a]

[a]CSIR-Institute of Microbial Technology, Chandigarh, India
[b]National Institute of Immunology, New Delhi, India

ABSTRACT A hallmark feature of *Mycobacterium tuberculosis* pathogenesis lies in the ability of the pathogen to survive within macrophages under a stressful environment. Thus, coordinated regulation of stress proteins is critically important for an effective adaptive response of *M. tuberculosis*, the failure of which results in elevated immune recognition of the tubercle bacilli with reduced survival during chronic infections. Here, we show that virulence regulator PhoP impacts the global regulation of heat shock proteins, which protect *M. tuberculosis* against stress generated by macrophages during infection. Our results identify that in addition to classical DNA-protein interactions, newly discovered protein-protein interactions control complex mechanisms of expression of heat shock proteins, an essential pathogenic determinant of *M. tuberculosis*. While the C-terminal domain of PhoP binds to its target promoters, the N-terminal domain of the regulator interacts with the C-terminal end of the heat shock repressors. Remarkably, our findings delineate a regulatory pathway which involves three major transcription factors, PhoP, HspR, and HrcA, that control *in vivo* recruitment of the regulators within the target genes and regulate stress-specific expression of heat shock proteins via protein-protein interactions. The results have implications on the mechanism of regulation of PhoP-dependent stress response in *M. tuberculosis*.

IMPORTANCE The regulation of heat shock proteins which protect *M. tuberculosis* against stress generated by macrophages during infection is poorly understood. In this study, we show that PhoP, a virulence regulator of the tubercle bacilli, controls heat shock-responsive genes, an essential pathogenic determinant of *M. tuberculosis*. Our results unravel that in addition to classical DNA-protein interactions, complex mechanisms of regulation of heat shock-responsive genes occur through multiple protein-protein interactions. Together, these findings delineate a fundamental regulatory pathway where transcription factors PhoP, HspR, and HrcA interact with each other to control stress-specific expression of heat shock proteins.

KEYWORDS global regulation, heat shock repressors, heat shock response, *M. tuberculosis* PhoP, protein-protein interactions

A hallmark feature of tuberculosis (TB) pathogenesis lies in the ability of the pathogen to survive within macrophages under a stressful environment. One of the pathways by which *Mycobacterium tuberculosis* survives exposure to unfavorable conditions encountered within the host involves the induction of a strong stress protein response following phagocytosis (1, 2). During infection, heat shock proteins, as a member of the major stress protein families, are induced in both the host and the pathogen to maintain cellular integrity and to contribute to immune signaling for recognition of the pathogen (3). In fact, elevated expression of heat shock proteins is necessary for bacterial adaptation to inhospitable conditions during intracellular growth and for survival of the bacilli. Thus, the

Citation Sevalkar RR, Arora D, Singh PR, Singh R, Nandicoori VK, Karthikeyan S, Sarkar D. 2019. Functioning of mycobacterial heat shock repressors requires the master virulence regulator PhoP. J Bacteriol 201:e00013-19. https://doi.org/10.1128/JB.00013-19.

Editor Victor J. DiRita, Michigan State University

Address correspondence to Dibyendu Sarkar, dibyendu@imtech.res.in.

* Present address: Ritesh Rajesh Sevalkar, Department of Microbiology, University of Alabama, Birmingham, Alabama, USA; Ranjeet Singh, The Energy and Resources Institute, New Delhi, India.

Received 5 January 2019
Accepted 1 April 2019
Accepted manuscript posted online 8 April 2019
Published 22 May 2019

pathogenesis of *M. tuberculosis* is significantly influenced by the regulatory expression of heat shock proteins. However, our knowledge of the underlying regulatory mechanism which couples heat shock conditions with global gene expression in *M. tuberculosis* remains superficial.

Although the pathogen does not encounter significantly increased temperature following the uptake of *M. tuberculosis* by host cells, heat shock proteins are induced possibly because bacterial adaptation to an inhospitable phagosome (during intracellular survival and growth) requires their elevated expression (4). In keeping with this, (i) heat shock proteins function to protect *M. tuberculosis* against stress generated by host macrophages during infection (5, 6) and (ii) partial disruption of heat shock regulation of *M. tuberculosis* strongly impacts virulence mechanisms, disabling the bacterium's ability to establish a chronic infection (4). Remarkably, DNA microarray experiments demonstrate that *acr2* (Rv0251c), which is a member of the α-crystallin family of molecular chaperone genes and which shows the highest activation during heat shock (4), is also the most upregulated gene following phagocytosis of *M. tuberculosis* by macrophages (2). Importantly, *acr2* expression remains essential for virulence in a murine model of tuberculosis (7). Thus, it is of interest to understand the molecular mechanism of regulation of heat shock-inducible gene expression of *M. tuberculosis*.

Although alternative sigma factors have been implicated in activation of *hsp70* expression (8), the major control of heat shock protein-encoding genes such as *hsp70-dnaK* is attributable to the release of transcriptional repression in a stress-specific manner (6). While canonical annotation of the *M. tuberculosis* genome shows the presence of two heat shock repressors, HspR and HrcA, deletion of *hspR* was of very little consequence on expression of *groE-hsp60* proteins (6). These results suggest that a second repressor *hrcA* locus in the genome plays an important role in the *M. tuberculosis* heat shock response. To investigate this, Stewart and coworkers compared whole-genome expression profiles of a Δ*hspR* strain and the double mutant Δ*hrcA* Δ*hspR* strain (4). Their results suggest that transcription control of a large number of heat shock-responsive genes is likely regulated by the *hrcA* locus as the major regulator. However, to date, the mechanism for regulating the heat shock-inducible genes of *M. tuberculosis* remains unknown.

Consistent with an overwhelming regulatory control by PhoP of approximately 2% of the genome, including the ESX-1 secretion apparatus (a major pathogenic determinant [9, 28]), mutations in *phoP* account for *in vivo* as well as *ex vivo* attenuation (9, 10). Previously, we showed that expression of *acr2*, a gene encoding a member of the widespread heat shock-inducible α-crystallin family of molecular chaperones which stabilize proteins during stress conditions, is dependent on the *phoP* locus (11). In this study, we wanted to investigate the impact of *phoP* on the *M. tuberculosis* transcriptome under heat shock conditions. Our microarray data implicate expression of numerous heat shock-responsive genes, including the essential chaperonin gene *groEL2*, by the *phoP* locus. Further probing highlighted the critical importance of protein-protein interactions involving PhoP as the nodal regulator and its mechanism of controlling stress-specific regulation of heat shock-responsive gene expression. Taking these findings together, we identify the most important regulatory circuits, showing interactions of PhoP with two heat shock repressors (HspR and HrcA) and how they coordinate mechanisms to transcriptionally control heat shock-responsive genes. Most importantly, consistent with the major regulatory involvement of PhoP as the nodal regulator, a Δ*phoP* variant displayed significantly higher heat shock-dependent cell death than wild-type (WT) bacilli.

RESULTS

***phoP* plays a global role in heat shock response of *M. tuberculosis*.** To examine whether *phoP* plays a global role in controlling heat shock response of *M. tuberculosis*, we performed microarray experiments using WT H37Rv and Δ*phoP* strains under both normal and heat shock conditions. Notably, the Δ*phoP* strain showed differential

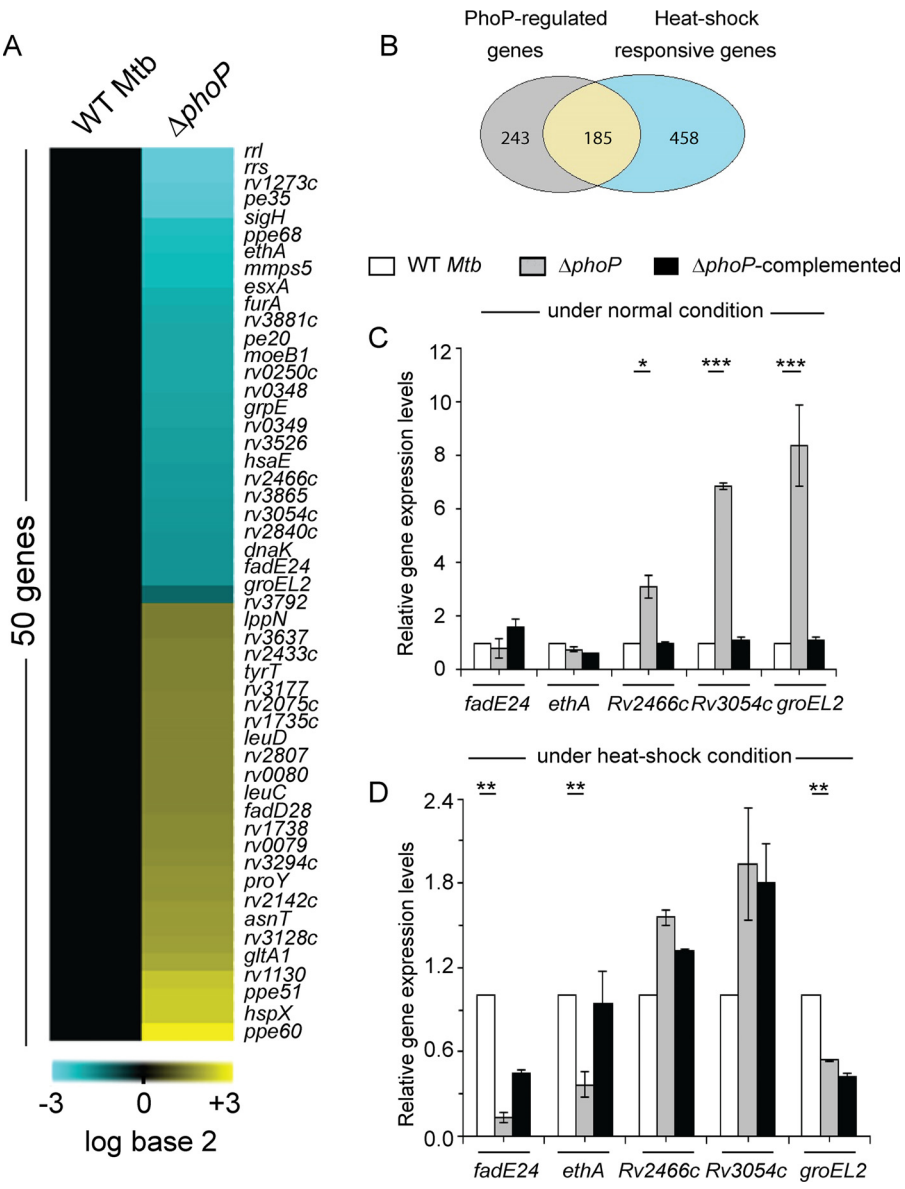

FIG 1 *phoP* locus is required for expression of heat shock-responsive genes of *M. tuberculosis*. (A) Heat shock-dependent levels of gene expression of WT and Δ*phoP* strains were compared by microarray experiments showing 50 significantly regulated genes from the cells grown with a heat shock at 45°C for 1 h 30 min. Cyan and yellow signify elevated or lowered gene expression, respectively, relative to WT *M. tuberculosis* grown under normal conditions (37°C). (B) Overlap of heat shock-responsive genes which displayed a ≥2-fold change in their expression in WT *M. tuberculosis* as a function of heat stress with genes which demonstrated ≥2-fold *phoP*-dependent differences of expression. Of the 643 heat shock-responsive genes, 185 were differentially regulated in the Δ*phoP* mutant. (C and D) Expression of heat shock-responsive genes in WT, Δ*phoP*, and Δ*phoP* complemented *M. tuberculosis* H37Rv grown with or without heat shock was examined by RT-qPCR as described in Materials and Methods. *, $P < 0.05$; **, $P < 0.01$; ***, $P < 0.001$. The average fold differences in expression levels with standard deviations from replicates were determined for at least three independent RNA preparations. The data reported in this study have been deposited in the NCBI's Gene Expression Omnibus (38) and are accessible through GEO series accession number GSE100596.

expression of a large fraction of the heat shock-responsive genes (Fig. 1A). Our results show that out of ~643 heat shock-responsive genes, approximately 185 are regulated by the *phoP* locus (Fig. 1B). Functional classification of these genes demonstrates a major impact of the *phoP* locus on diverse physiological functions, with the most-affected genes being for intermediary metabolism and respiration (see Fig. S1 in the supplemental material).

TABLE 1 Plasmids used in cloning reported in this study

Plasmid	Characteristic(s)	Source or reference
pET15b	*E. coli* cloning vector, Amp^{r}[a]	Novagen
pET-*hspR*	HspR residues 1–126 cloned in pET15b	This study
pET-*hrcA*	HrcA residues 1–343 cloned in pET15b	This study
pET15b-*hspR*Δ10	HspR residues 1–116 cloned in pET15b	This study
pET15b-*hrcA*Δ18	HrcA residues 1–325 cloned in pET15b	This study
pGEX-4T-1	*E. coli* cloning vector, Amp^{r}	GE Healthcare
pGEX-*hrcA*	HrcA residues 1–343 cloned in pGEXT-4T-1	This study
pGEX-*hspR*	HspR residues 1–126 cloned in pGEXT-4T-1	11
pGEX-*phoP*	PhoP residues 1–247 cloned in pGEX-4T-1	32
p19Kpro	Mycobacterial expression vector, Hyg^{r}[b]	14
p19Kpro-*phoP*	PhoP residues 1–247 cloned in p19Kpro	15
p19Kpro-*hrcA*	HrcA residues 1–343 cloned in p19Kpro	This study
pSTKi	Integrative mycobacterial expression vector, Kan^{r}[c]	13
pSTKi-*hrcA*	HrcA residues 1–343 cloned in pSTKi	This study
pSTKi-*hspR*	HspR residues 1–126 cloned in pSTKi	This study
pSTKi-*hrcA*Δ18	HrcA residues 1–325 cloned in pSTKi	This study
pSTKi-*hspR*Δ10	HspR residues 1–116 cloned in pSTKi	This study
pUAB300[b]	Episomal mycobacteria-*E. coli* shuttle plasmid	16
pUAB300-*hrcA*	HrcA residues 1–343 cloned in pUAB300	This study
pUAB300-*hspR*Δ10	HspR residues 1–116 cloned in pUAB300	This study
pUAB300-*hrcA*Δ18	HrcA residues 1–325 cloned in pUAB300	This study
pUAB400[c]	Integrative mycobacterium-*E. coli* shuttle plasmid	16
pUAB400-*phoP*	PhoP residues 1–247 cloned in pUAB400	11
pUAB400-*phoP*N	PhoP residues 1–141 cloned in pUAB400	This study
pUAB400-*phoP*C	PhoP residues 141–247 cloned in pUAB400	This study

[a]Amp^{r}, ampicillin resistant.
[b]Hyg^{r}, hygromycin resistant.
[c]Kan^{r}, kanamycin resistant.

To validate the microarray data, we next performed reverse transcriptase quantitative PCR (RT-qPCR) of a few representative *M. tuberculosis* genes (see Fig. S2). Table S1 lists the page-purified oligonucleotide primers used in the RT-qPCR experiments. In agreement with the microarray data, we observed significantly higher expression of three heat shock-inducible genes (*Rv2466*, *Rv3054*, and *groEL2*) in the Δ*phoP* strain relative to that in WT bacteria under normal conditions (Fig. 1C). We next compared the expression of these genes relative to that in WT bacteria during heat stress (Fig. 1D). Strikingly, we found significantly lower expression of *fadE24*, *ethA*, and *groEL2* in the Δ*phoP* mutant than in WT *M. tuberculosis*. These results suggest that *phoP* plays a major role in heat shock-dependent activation of gene expression. Together, consistent with the microarray data, the RT-qPCR experiments reveal that a large number of heat shock-responsive genes are regulated by the *phoP* locus.

Repression of heat shock-inducible genes. Next, we utilized "mycobacterial recombineering" (12) to construct Δ*hrcA* and Δ*hspR* strains (see Fig. S3A and B) to probe the mechanism of regulation. The mutants were verified by gene-specific PCR using corresponding genomic DNA as PCR templates (Fig. S3C and D, respectively; Table S2 lists relevant oligonucleotide primers used in cloning, and Table 1 shows the plasmid constructs used in this study). The genomic DNA of the Δ*hrcA* strain showed the unique presence of a 1.3-kb *hyg* cassette, while the *hrcA* gene product was absent (Fig. S3C, compare lane 3 and lane 2). In contrast, the complemented mutant, which utilized the integrative pSTKi (13) harboring a copy of the *hrcA* gene, showed the presence of both the gene-specific product and the *hyg* cassette (lane 4). Likewise, *hspR*-specific amplification from the genomic DNA of the Δ*hspR* strain yielded similar results (Fig. S3D). Furthermore, we verified the mutant constructs by Southern blot analyses (Fig. S3E). In the Southern blot analysis, WT *M. tuberculosis* showed two specific bands of approximately 10 and 8.3 kb when probed with *hrcA*- and *hspR*-specific probes, respectively. Hybridization of Δ*hrcA* genomic DNA using identical probes detected an *hspR*-specific band (~8.3 kb) only. In contrast, only the *hrcA*-specific product (~10 kb) was detectable in the Δ*hspR* mutant-derived genomic DNA. Our additional RT-qPCR experiments

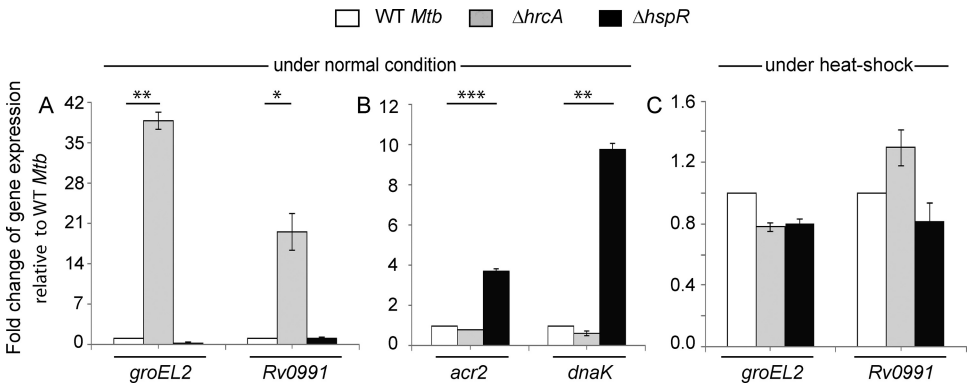

FIG 2 Both HrcA and HspR function as major heat shock repressors. mRNA levels of indicated genes were determined by RT-qPCR in WT and mutant bacteria under normal (A and B) and heat shock (C) conditions of growth, as described in the legend for Fig. 1C and D. The results unambiguously demonstrate specific regulatory effects of the repressors; panel C shows comparable levels of expression of heat shock-inducible genes under heat stress. In all cases, the average fold differences in expression levels with standard deviations from replicate experiments were determined from at least three independent RNA preparations.*, $P < 0.05$; **, $P < 0.01$; ***, $P < 0.001$.

showed that while mRNA levels of *hrcA* and *hspR* remained undetectable in the corresponding mutants (Fig. S3E and F), their expressions in the correspondingly complemented strains were largely restored to the WT level. Table S3 lists the strains used in this study.

Previous studies by Stewart and coworkers showed that while HrcA functions as a regulator of *groEL2* and *Rv0991*, HspR controls expression of *acr2* and *dnaK* expression in *M. tuberculosis* (4). In agreement with these results, we observed a significant activation of *groEL2* and *Rv0991* expression in the Δ*hrcA* strain under normal conditions (Fig. 2A); however, the WT and Δ*hspR* strains showed comparable *groEL2* expression. Further corroborating our previous results (11), we observed a strong upregulation of *acr2* and *dnaK* expression in the Δ*hspR* strain but not in the WT and the Δ*hrcA* mutant (Fig. 2B). Thus, genes which were not repressed in the Δ*hrcA* mutant showed WT-like repression in the Δ*hspR* mutant, and genes which were not repressed in the Δ*hspR* mutant showed WT-like repression in the Δ*hrcA* mutant. These results confirm that (i) the two genome-encoded heat shock repressors function independently of their respective regulons and (ii) the genes belonging to either HspR or HrcA regulon are targets of PhoP. In line with the general mechanism of repressor function, under heat shock conditions, both the WT and the mutants showed comparable levels of expression of heat shock-inducible genes (Fig. 2C).

***In vivo* recruitment of regulators.** Although by chromatin immunoprecipitation (ChIP)-qPCR we were unable to observe significant recruitment of PhoP within a majority of its target promoters, our results showed effective PhoP recruitment within the *groEL2* promoter, under both normal and heat shock conditions (Fig. 3A). These results are consistent with the presence of a likely PhoP binding motif (−127 to −112, relative to the translational start site) within the *groEL2* regulatory region. While we presume an indirect role of the *phoP* locus for other heat shock-responsive genes, *in vivo* binding results are in agreement with regulation data under both normal and stress conditions (Fig. 1). Next, to determine HrcA recruitment, the repressor was expressed as a FLAG-tagged protein, and ChIP experiments were carried out using an anti-FLAG antibody (Thermo) (as described in Materials and Methods). As expected, we found considerable recruitment of HrcA within the *groEL2* promoter of WT *M. tuberculosis* (Fig. 3B). However, HrcA recruitment was insignificant under heat shock conditions, suggesting derepression of promoter activity during stress (Fig. 2C). Figure 3C shows a schematic presentation of the *groEL2* regulatory region comprising newly identified PhoP and previously reported HrcA binding sites (4). Note that our attempt to examine the formation of a ternary (PhoP-groEL2up-HrcA) complex was unsuccess-

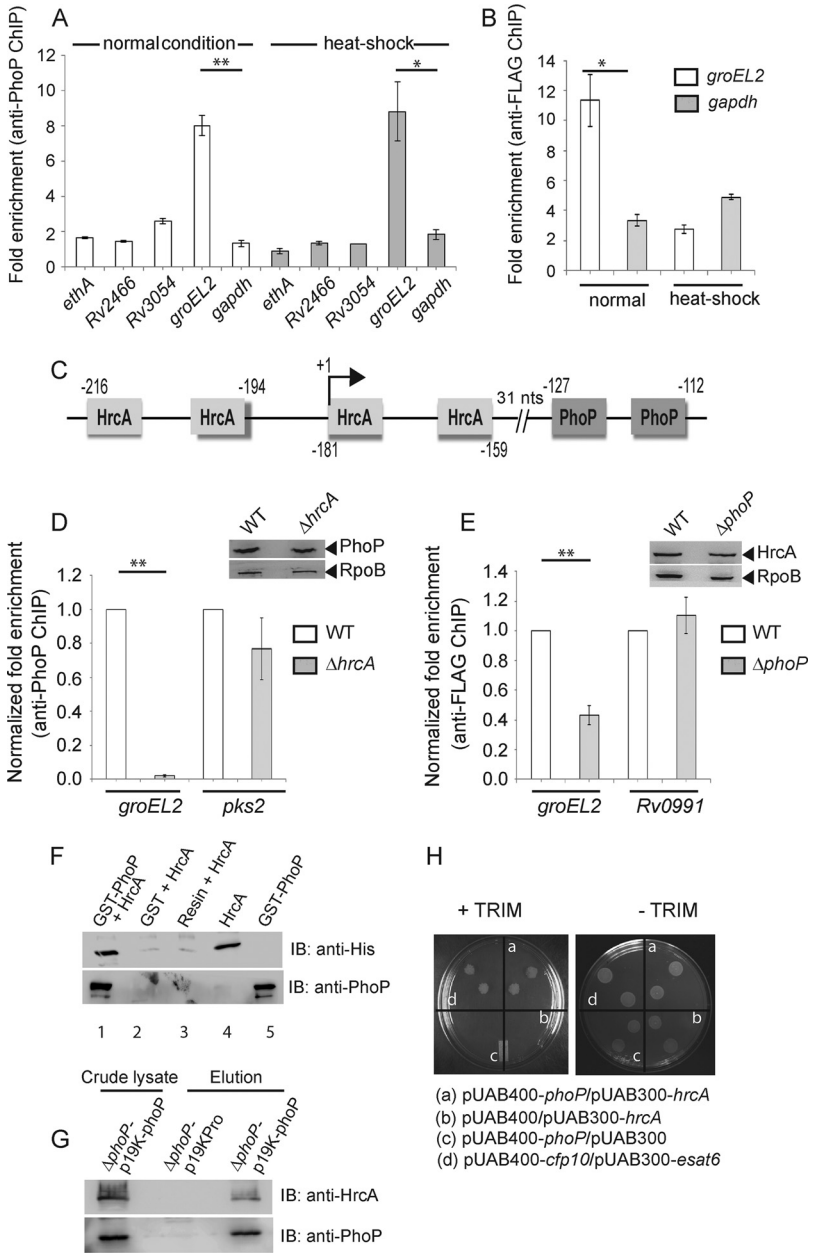

FIG 3 *In vivo* recruitment of regulators. (A) Recruitment of PhoP within heat shock-responsive genes, under both normal and heat shock conditions, was investigated by ChIP-qPCR using anti-PhoP antibody (Alpha Omega Sciences) as described previously (24). (B) To examine HrcA recruitment within groEL2up, FLAG-tagged HrcA was expressed in WT *M. tuberculosis* (see Materials and Methods), and ChIP-qPCR was carried out using anti-FLAG antibody (Thermo Scientific). (C) Schematic presentation of the newly identified PhoP and previously reported HrcA binding sites (4) within the *groEL2* regulatory region. The locations of binding sites are indicated by nucleotide positions relative to the translational start site of *groEL2*. The transcription start site (+1) is shown by an arrow. (D and E) To compare *in vivo* recruitments of PhoP in WT and Δ*hrcA* strains (D) and HrcA in WT and Δ*phoP* strains (E), fold enrichments were determined relative to the PCR signal from mock IP sample without adding antibody. Insets show comparable PhoP and HrcA expression in crude cell lysates of indicated mutants containing 10 μg of total protein; RpoB was used as the loading control. (F) To examine PhoP-HrcA interaction *in vitro*, crude extract expressing His_6-tagged HrcA was incubated with glutathione-Sepharose previously immobilized with GST-PhoP. Fractions of bound proteins (lane 1) were analyzed by Western blotting using anti-HrcA (top) or anti-PhoP (bottom) antibody. As controls, glutathione-Sepharose was immobilized with GST alone (lane 2) or the resin alone (lane 3); lanes 4 and 5 resolved purified HrcA and GST-PhoP, respectively. (G) To confirm PhoP-HrcA interaction *in vivo*, crude cell lysates of the Δ*phoP* mutant expressing His_6-tagged PhoP (p19Kpro-*phoP*) (Table 1) were incubated with preequilibrated Ni-NTA and eluted with 250 mM imidazole; left lane, input sample; middle lane, control elution from the crude lysate of cells lacking *phoP* expression; right lane, *M. tuberculosis* HrcA showing coelution with PhoP. (H) M-PFC

(Continued on next page)

ful, since PhoP and/or HrcA was ineffective in forming a complex stable for gel electrophoresis.

Having shown recruitment of both PhoP and HrcA within the *groEL2* promoter, we investigated whether that recruitment of the regulators is linked. In ChIP experiments, we observed a significant reduction of PhoP recruitment within the *groEL2* regulatory region of the Δ*hrcA* strain relative to that for the WT bacteria (Fig. 3D). However, PhoP recruitments within the *pks2* promoter (regulated by PhoP but not by HrcA) remained comparable between the WT and the mutant. The inset in the figure shows comparable levels of *phoP* expression in WT and the Δ*hrcA M. tuberculosis*. Likewise, HrcA recruitment within the *groEL2* regulatory region but not *Rv0991* (which is regulated by HrcA but not by PhoP) was significantly reduced in the Δ*phoP* mutant relative to that in WT bacteria (Fig. 3E). Thus, we conclude that the presence of both *hrcA* and *phoP* is necessary for effective recruitment of PhoP and HrcA, respectively, within the target promoter. Unfortunately, this experiment could not be extended to other heat shock-responsive promoters, as we were unable to observe a significant fold enrichment in ChIP-qPCR studies using anti-PhoP antibody (Fig. 3).

Having noted this link, we attempted an *in vitro* pulldown assay to investigate whether HrcA interacts with PhoP. In this experiment, glutathione transferase (GST)-PhoP was immobilized on glutathione-Sepharose followed by incubation with purified recombinant HrcA. Upon elution of column-bound proteins, we detected the presence of both proteins in the same fraction (Fig. 3F, lane 1). However, an identical experiment with only the GST tag (lane 2) or the resin alone (lane 3) did not detect HrcA, suggesting that PhoP interacts with HrcA. In an *in vivo* experiment, His-tagged PhoP was expressed in the Δ*phoP* mutant using the p19Kpro expression vector (14) as described previously (15). The cell lysate (Fig. 3G, input sample, left lane) was incubated with Ni-nitrilotriacetic acid (Ni-NTA) beads, and following multiple washings with the binding buffer, bound proteins were eluted with imidazole. While the eluent showed the clear presence of HrcA (third lane), we were unable to detect HrcA from the cell lysate of the Δ*phoP* mutant carrying p19Kpro (empty vector control, second lane), suggesting specific interactions between PhoP and HrcA *in vivo*. We next utilized a previously reported mycobacterial protein fragment complementation assay (M-PFC) (16), in which the bait and prey plasmids were prepared as C-terminal fusions with complementary fragments of mDHFR (Table 1; see Materials and Methods). Next, *Mycobacterium smegmatis* transformants were selected on 7H10-kanamycin (Kan)-hygromycin (Hyg) plates either in the presence or in the absence of 15 μg/ml trimethoprim (TRIM). Although cells harboring empty vectors did not show any growth on 7H10-TRIM plates, cells coexpressing PhoP/HrcA grew well in the presence of TRIM (Fig. 3H). Together, the M-PFC results are consistent with the above *in vitro* and *in vivo* data to suggest that PhoP interacts with HrcA.

Probing PhoP-heat shock repressor protein-protein interactions. As structural data are not available, HspR and HrcA structures were predicted using the Phyre2 Web portal (17) (see Fig. S4 and S5, respectively). Using PDB identifier (ID) 3D6Z (18) as the template, Phyre2 predicted an HspR structure with 99.85% confidence, and a HrcA structure was predicted at a 90% confidence level using the PDB ID 1STZ (19) as the template. To probe the interaction(s) further, we docked HspR and HrcA structures individually onto the complete PhoP-DNA complex (PDB ID 5ED4) using the ZDock server (20). Based on the score, the ZDock predicted 10 different conformations of the PhoP-DNA-HspR complex. Strikingly, the structural analysis revealed that 7 of 10 conformations show a common binding site of HspR to the PhoP-DNA complex (see

FIG 3 Legend (Continued)
experiment to examine the PhoP and HrcA interaction involved coexpression of indicated fusion constructs in *M. smegmatis*. Growth of transformants on 7H11-Kan-Hyg in the presence of TRIM indicated *in vivo* protein-protein association between PhoP and HrcA. Coexpression of empty vectors and the esat6-*cfp10* pair were included as negative and positive controls, respectively. All of these strains grew well in the absence of TRIM. **, $P < 0.01$; *, $P < 0.05$.

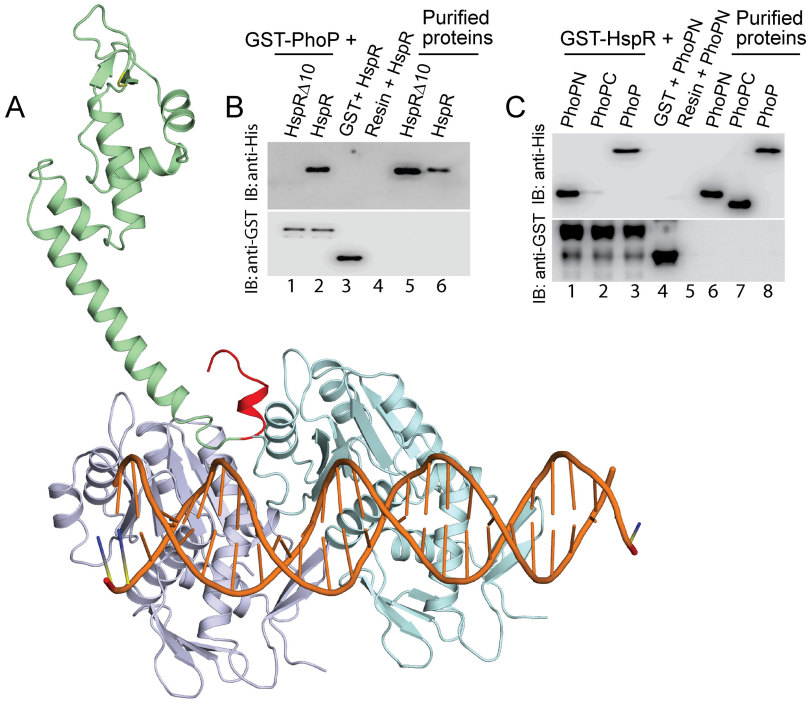

FIG 4 Docking of HspR structure on PhoP-DNA complex. (A) The docking of HspR structural model on PhoP-DNA complex utilized a submission of the respective structural coordinates to the docking server ZDock (20) as detailed in Results. (B) To examine the role of the C-terminal 10 residues of HspR (shown in red in panel A) in PhoP-HspR interactions, crude lysates of cells expressing His_6-tagged HspRΔ10 were incubated with glutathione-Sepharose, previously immobilized with GST-PhoP. Fractions of bound proteins (lane 1) were analyzed by Western blotting using anti-His (top) or anti-GST (bottom) antibody. Control sets include glutathione-Sepharose immobilized with GST alone (lane 3) or the resin alone (lane 4); lanes 5 and 6 resolve purified HspRΔ10 and HspR, respectively. (C) *In vitro* interactions of HspR and indicated PhoP domains (PhoPN and PhoPC) were investigated by incubating crude cell lysates of His_6-tagged PhoP domains with glutathione-Sepharose previously immobilized with GST-HspR. The results suggest that the PhoPN, and not PhoPC, retains the ability to interact with HspR (see Results for more details). Note that PhoP N and PhoP C domain constructs, used in this study, were previously shown to be fully functional on their own (21).

Fig. S4), thus generating a consensus binding pattern (Fig. 4A). However, despite predicting 10 different conformations, a consensus binding model was not apparent upon structural docking of HrcA onto the PhoP-DNA complex (Fig. S5). Considering the structural complexity of the macromolecular complex and limitations of "rigid body docking," the above failure might be attributable to limitations of the prediction method. However, a closer inspection of the structural model of the HspR-PhoP-DNA complex suggests that the C-terminal region of HspR interacts with the N-terminal region of PhoP (Fig. 4A).

To examine the accuracy of the predicted structural model, we analyzed the *in vitro* interactions between recombinant His-tagged HspRΔ10, lacking C-terminal 10 residues (residues 126 to 143) of HspR, with the GST-PhoP as described previously (11). Upon elution of column-bound proteins, we were unable to detect the presence of both PhoP and HspRΔ10 proteins in the same fraction (Fig. 4B, lane 1). However, under identical conditions, we detected both PhoP and full-length HspR in the same fraction (lane 2), suggesting that the PhoP-HspR interaction involves C-terminal residues of HspR. *In vitro* DNA binding assays with the purified WT and truncated proteins (as shown in Fig. S6A) suggested structural integrity of the truncated variant (Fig. S6B). As expected, in the M-PFC experiments, PhoP failed to demonstrate protein-protein interaction with HspRΔ10, the truncated repressor (Fig. S6C). From these results, we speculate that not a few residues in a stretch but possibly a constellation of amino acids contribute to protein-protein interactions.

Having confirmed the accuracy of the model showing possible interaction between PhoP and the C-terminal end of HspR, we next assessed the role of different stretches of the PhoP N domain in PhoP-HspR interactions. During *in vitro* pulldown assays with GST-HspR, mutant PhoP proteins (each with three potential HspR-contacting residues replaced with Ala) showed protein-protein interactions as effectively as WT PhoP (Fig. S7A). We next sought to probe the PhoP-HspR interaction using truncated PhoP domains, previously shown to be functional on their own (21). During *in vitro* experiments, PhoPN, comprising N-terminal PhoP residues 1 to 141, showed an effective protein-protein interaction with HspR (Fig. 4C, lane 1); however, PhoPC (comprising C-terminal PhoP residues 141 to 247), under identical conditions, failed to show an effective interaction with HspR (lane 2). To further confirm these results, we performed M-PFC experiments. As expected, cells coexpressing PhoPN and HspR but not PhoPC/HspR (Fig. S7B) supported *M. smegmatis* growth in the presence of TRIM. Taking these results together, we conclude that PhoPN interacts with the C-terminal end of HspR. It is noteworthy that the C-terminal hydrophobic tail of HspR is also known to be required for DnaK-assisted HspR functioning as a DNA binding transcriptional repressor (22).

With the evidence showing the N domain of PhoP interacts with HspR, we next probed the PhoP-HrcA interaction more closely. Based on the HrcA structural model (Fig. 5A), we designed HrcAΔ18, a C-terminal truncated mutant of HrcA comprising amino acid residues 1 to 325 (Table 1). *In vitro* pulldown studies using GST-PhoP and truncated HrcA (His-tagged) (as described in Fig. 4B) suggest the C-terminal 18 residues of HrcA are essential for PhoP-HrcA interactions (Fig. 5B). These results were further confirmed by additional M-PFC experiments (Fig. 5C). Together, these results establish the specificity of PhoP-HrcA interactions. To examine the effect of C-terminal truncation of HrcA on its regulatory activity, we compared expression of *groEL2* and that of *Rv0991* (target genes of HrcA) (Fig. 2G) in a Δ*hrcA* strain complemented with truncated HrcA and the full-length HrcA, respectively (Fig. 5D). Strikingly, HrcAΔ18, unlike full-length HrcA, only partially complemented *groEL2* expression. However, Rv0991 expression, which remains independent of PhoP-HrcA interactions, was restored by either of the two proteins. Thus, in conjunction with the above results, we conclude that the regulation of *groEL2* expression requires PhoP-HrcA interaction, the lack of which accounts for the failure to restore *groEL2* expression level in the Δ*hrcA*::*hrcA*Δ18 mutant (but not in the Δ*hrcA*::*hrcA* strain). Taken together with *in vitro*, *ex vivo*, and *in vivo* findings, these results suggest a pathway in which the interaction between a pair of repressors with a common nodal regulator controls the expression of specific heat shock-dependent genes.

To further probe the PhoP-HrcA interaction, we next used purified PhoP domains (His tagged) and GST-HrcA (as described in Fig. 4C). Our results unambiguously prove that similar to HspR (11), PhoPN shows effective protein-protein interaction with HrcA (Fig. 5E). The results were also validated by M-PFC experiments using the full-length regulator pair as positive control (Fig. 5F). Taking these results together, we conclude the PhoP N domain also interacts with the C-terminal end of HrcA, the other *M. tuberculosis* heat shock repressor. An effort to quantify interaction affinity using alamarBlue at multiple TRIM concentrations yielded confusing results, possibly because of interference from HrcA and/or HspR homologs of *M. smegmatis*.

With a global impact of the *phoP* locus on the *M. tuberculosis* transcriptome (related to heat shock-responsive genes), we next investigated the impact of *phoP* on *M. tuberculosis* physiology under heat stress. Thus, we studied the role of the *phoP* locus on survival of the tubercle bacilli under heat stress. We exposed WT *M. tuberculosis* and the Δ*phoP* and complemented mutant strains to 45°C for various lengths of time and examined their survival by CFU plating (Fig. 6). We observed that the Δ*phoP* mutant was significantly more susceptible to heat shock than the WT strain (compare 48% ± 2% survival of the mutant versus 71% ± 5% survival of the WT bacilli grown under 6 h of heat shock). However, the Δ*phoP* complemented strain, under identical conditions, showed comparable survival to that of the WT bacilli. In keeping with the regulatory

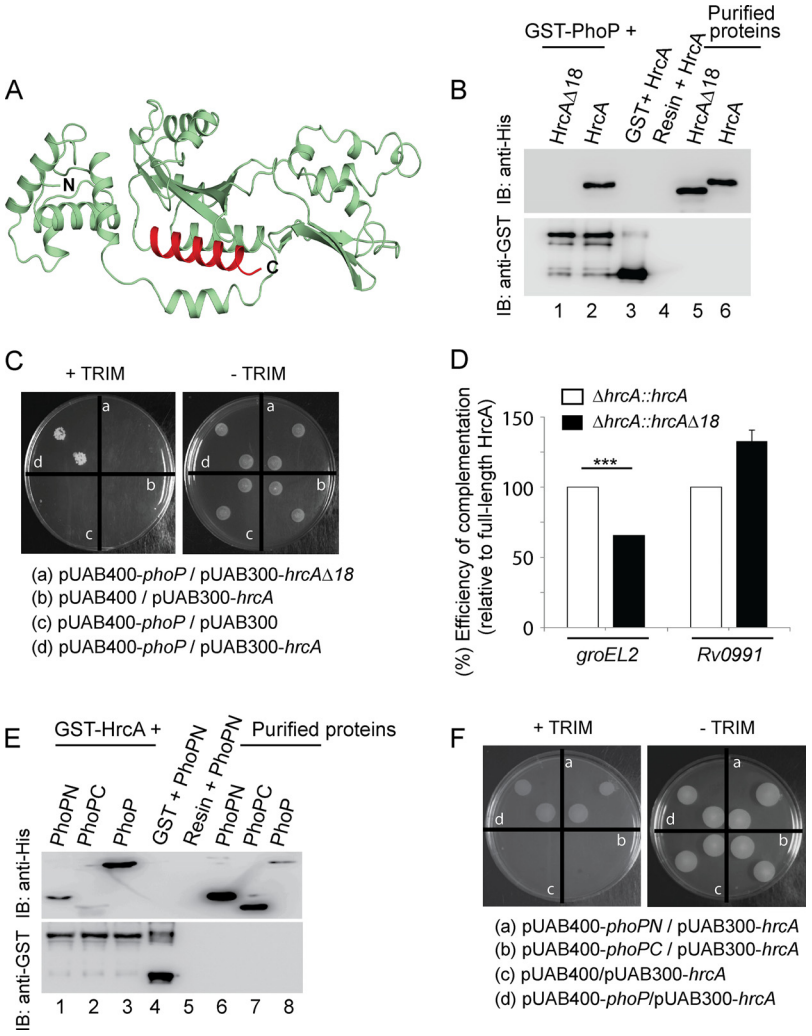

FIG 5 C-terminal end of HrcA interacts with the N-terminal domain of PhoP. (A) The HrcA structural model showing the C-terminal truncation (shown in red) was generated as described in Results. (B) To assess the importance of the C-terminal 18 residues of HrcA in PhoP-HrcA interactions, crude lysates of cells expressing His_6-tagged HspRΔ10 were incubated with glutathione-Sepharose previously immobilized with GST-PhoP, and samples were analyzed as described in the legend for Fig. 4B. (C) M-PFC experiment to examine interaction between PhoP and truncated HrcA involved coexpression of indicated fusion constructs (including PhoP and HrcA as the positive control) in *M. smegmatis* as described in the legend for Fig. 3G. (D) Restoration of expression of indicated genes in the Δ*hrcA* mutant was examined via RT-qPCR by complementing with either the full-length or the truncated *hrcA* gene. The results suggest *in vivo* relevance of the C-terminal end of HrcA, a region involved in protein-protein interactions with PhoP. As a control, regulation of *phoP*-independent *Rv0991* expression by the truncated HrcA remained unaffected. (E) *In vitro* interactions of HrcA and indicated PhoP domains (PhoPN and PhoPC) were investigated by incubating crude cell lysates of His_6-tagged PhoP domains with glutathione-Sepharose previously immobilized with GST-HrcA. The results suggest that PhoPN, and not PhoPC, retains the ability to interact with HspR (see Results for more details). (F) M-PFC experiments to examine the interaction between HrcA and indicated PhoP domains involved coexpression of indicated fusion constructs (including PhoP and HrcA as the positive control) in *M. smegmatis* as described in the legend for Fig. 3G.

role of the *phoP* locus, these results demonstrate that *phoP* plays a major role in the survival of *M. tuberculosis* under heat shock conditions.

DISCUSSION

The results reported in this study provide new biological insights into how virulence-associated *phoP* plays a global role in the regulation of heat shock-responsive gene expression. We identify a new protein-protein interaction between PhoP and one of the heat shock repressors, HrcA, which is required for the repression of heat shock-

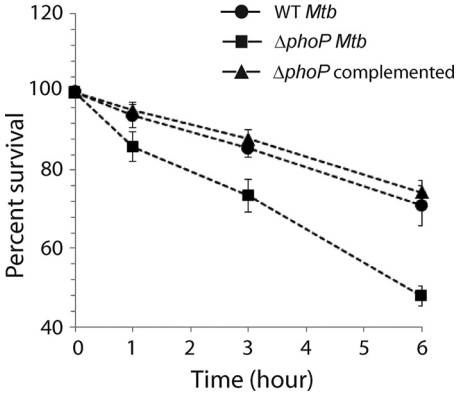

FIG 6 Deletion of *phoP* from *M. tuberculosis* H37Rv reduces its survivability under heat stress. WT and Δ*phoP M. tuberculosis* strains were compared for survival under increasing heat stress by CFU counting ($n = 3$). Although the Δ*phoP* strain grew comparably well as the WT bacilli under normal conditions, it remained significantly growth defective under heat stress. However, the growth defect of the mutant was completely restored in the complemented mutant. Note that 100% survival of the bacilli is assumed at the zero time point.

inducible genes under normal conditions. These results are not merely an extension of the previously studied heat shock-specific *acr2* regulation for the following reasons. First, our results comprise the first account of global regulation of the heat shock response in *M. tuberculosis*. Second, independent functioning of the two genome-encoded heat shock repressors (HspR and HrcA) has been shown clearly. The third and perhaps most interesting finding highlights the role of the virulence regulator PhoP as a common requirement for effective functioning of both heat shock repressors via specific protein-protein interactions. We further demonstrate that effective interactions involve the N-terminal domain of PhoP and the C-terminal end of heat shock repressors. We postulate that PhoP-repressor protein-protein interactions, in addition to their respective DNA binding functions, regulate the expression of specific heat shock-inducible genes in *M. tuberculosis*. Together, these results account for the lowered survival of the Δ*phoP* strain relative to the WT bacilli under increasing heat stress.

Having shown the roles of both PhoP and HrcA in regulating heat shock-responsive genes (Fig. 1 and 2), we next considered whether these regulators are functionally connected. Our results demonstrate that PhoP-HrcA protein-protein interaction accounts for concomitant binding of both the regulators as corepressors of *groEL2* expression (Fig. 3). These results take on more significance in light of the previous finding that PhoP and HspR function as corepressors of heat shock-inducible *acr2* expression (11). We further utilized Δ*hrcA* and Δ*hspR* mutants in our *in vivo* regulatory studies to determine that *phoP*, *hrcA*, and *hspR* loci together coordinate a global role in heat shock-inducible gene expression. What offers a new mechanistic insight is the finding that the regulation of a specific set of heat shock-inducible genes is dependent on multiple protein-protein interactions, with PhoP as the common transcriptional regulator. We propose that the availability of repressor (HspR or HrcA) binding sites within the target promoters most likely determines which interaction, at any given time, is more relevant.

Notably, PhoP-HrcA-*groEL2* regulation follows a hybrid model and is clearly different from the PhoP-HspR-*acr2* regulatory scheme. This is because while PhoP and HrcA function as corepressors of *groEL2* expression under normal conditions (Fig. 1C and 2A, respectively), during heat shock, PhoP activates *groEL2* expression (Fig. 1D) without any assistance from HrcA (Fig. 2A). Although this model is consistent with PhoP binding to the *groEL2* promoter under both normal and stress conditions (Fig. 3A), this situation is unlike the regulation of *acr2* expression, where both PhoP and HspR bind and leave the target site together (11). Therefore, PhoP appears to be interacting with HrcA only under normal conditions. However, there are two apparent contradictions. First, while

the presence of HrcA is essential for PhoP recruitment under normal conditions (Fig. 3D), how is PhoP recruited within the *groEL2* promoter under heat stress (Fig. 3A) in the absence of HrcA (Fig. 3B)? The second related issue concerns the mechanism of activation of gene expression by PhoP under heat shock conditions. The question remains whether what we observed in the Δ*phoP* mutant is attributable to *phoP*-dependent activation or whether it is due to the absence of a functional PhoP-HrcA interaction leading to derepression of target promoter activity. From the observations that (i) *groEL2* is expressed at a significantly lower level in the Δ*phoP* strain (relative to WT *M. tuberculosis*) only under heat shock conditions and (ii) PhoP shows recruitment within *groEL2* promoter under heat stress (even in the absence of HrcA), we propose that PhoP functions as a specific activator of *groEL2* expression during heat stress. While we cannot rule out the possibility of PhoP functioning independently under heat shock conditions, two explanations might account for PhoP functioning during heat stress. Either there is involvement of another protein/factor along with PhoP under heat shock conditions or the regulator during stress undergoes a conformational change which provides the binding energy so that it can now bind to the target promoter(s) on its own.

While the DNA binding mechanism of PhoP is well known (23), our knowledge of protein-protein interactions involving the major virulence regulator has been limited to a few examples (15, 24). Thus, biochemical studies are required to identify newer working partners of the regulator. Having identified HspR (11) and HrcA (this study) as functional partners of PhoP, we attempted to decipher the origin of binding specificity. Our structure-guided docking results provide new insights into the protein-protein interaction that remain unavailable from the structural data alone. Although we cannot rule out the possibility of involvement of other regions of PhoP, here, we identified specific interactions between the PhoP N domain and both HspR and HrcA (Fig. 4 and 5, respectively). Thus, the likelihood that the interactions are nonspecific seems very low. However, we were unable to observe simultaneous recruitment of both PhoP and HrcA using an electrophoretic mobility shift assay (EMSA) as we had previously demonstrated in PhoP-HspR-*acr2* regulatory scheme (11). Therefore, it is arguable whether both the regulators are bound to *groEL2* promoter (at the same time) resulting in DNA looping. We suggest the following explanations that support the proposed mechanism. First, the *in vivo* recruitment of PhoP and HrcA under normal conditions was dependent on each other (Fig. 3). Second, the binding site of PhoP within the promoter was ~50 bp away from the HrcA binding site (4) (Fig. 3C), a result which is analogous to PhoP and HspR recruitment within ~50 bases of the *acr2* promoter (11) and consistent with DNA looping. Finally, the fact that the DNA binding functions are restricted to the C domain of PhoP (21) and N domain of HspR/HrcA (25, 26), these results showing interactions between PhoP N domain and the repressor (HspR/HrcA) C domains are remarkably consistent with our previously proposed model postulating PhoP-HspR functioning as corepressors (11).

The results showing activation of *groEL2*, an essential chaperonin gene (27), by the *phoP* locus during heat shock stress suggest that the presence of *phoP* is required for *groEL2* activation (Fig. 1D). Consistent with this result, unlike *acr2* regulation, even under heat shock conditions, PhoP is recruited within the regulatory region of *groEL2* (Fig. 3A). These results are in keeping with the higher sensitivity of the mutant strain (relative to the WT bacilli) to increasing heat stress. Notably, while the Δ*phoP* mutant showed considerably higher susceptibility to heat shock than WT bacteria, complementation of the mutant bacilli restored the bacterial survival pattern to the WT level. Although we cannot rule out the possibility of another PhoP-dependent mycobacterial response impacting the survival phenotype of the mutant under heat stress conditions, the above results showing *phoP*-dependent regulation of a large number of heat shock-responsive genes most likely through specific interactions with both the mycobacterial heat shock repressors facilitate an integrated view of our results. Together, these findings provide new mechanistic insights of striking significance into the regulation of heat shock-responsive *groEL2* of *M. tuberculosis*.

MATERIALS AND METHODS

Bacterial strains and culture conditions. *E. coli* DH5α and *E. coli* BL21(DE3) strains were grown at 37°C in LB medium containing appropriate antibiotics and used for cloning and for overexpression of mycobacterial proteins, respectively. The Δ*phoP* and complemented mutants were described previously (28). The construction of the Δ*hspR* and Δ*hrcA* strains and the complemented mutants is described below. *M. tuberculosis* strains, as listed in Table S3 in the supplemental material, were grown aerobically at 37°C in Middlebrook 7H9 liquid broth (containing 0.2% glycerol, 0.05% Tween 80, and 10% albumin-dextrose-catalase [ADC]) or on 7H10 agar medium (containing 0.5% glycerol and 10% oleic acid-albumin-dextrose-catalase [OADC]). For heat shock stress, *M. tuberculosis* was grown as described previously (11). Transformation of wild-type (WT) and mutant *M. tuberculosis* strains and selection of transformants on appropriate antibiotics were carried out as described previously (29).

RNA isolation and microarray analysis. Total RNA from *M. tuberculosis* grown in 7H9 medium was isolated and purified as described elsewhere (30). Briefly, 25 ml of bacterial culture of each strain was grown to mid-log phase (optical density at 600 nm [OD_{600}] of 0.4 to 0.6) at 37°C in 7H9 medium (pH 7.0) containing 10% ADC with shaking at 90 rpm. In each case, the cultures were divided in half; the first half was used as a control and the other half of the cultures was subjected to heat shock at 45°C for 1 h 30 min. This was followed by the addition of 75 ml 5 M guanidinium thiocyanate (GTC), 25 mM sodium citrate, 1% β-mercaptoethanol, and 0.5% Tween 80. Cells were pelleted by centrifugation, washed twice with phosphate-buffered saline (PBS), and lysed by resuspending in acetate-EDTA buffer (10 mM Na-acetate, 2 mM EDTA) containing acid-washed glass beads (one-sixth of the final volume; Sigma), 2% SDS, and acid-saturated phenol (pH 4.5) (Ambion). Following incubation at 65°C for 30 min, with intermittent vortexing (3 $\times$ 20 s) every 10 min, total RNA was extracted with chloroform-isoamyl alcohol and precipitated with chilled ethanol. To remove genomic DNA, RNA was treated with RNase-free DNase I (Invitrogen) for 20 min at room temperature; the quality of RNA samples was assessed by intactness of 23S and 16S rRNA using formaldehyde-agarose gel electrophoresis, and RNA concentrations were determined by measuring the absorbance at 260 nm.

For microarray analysis, the purity and integrity of RNA were examined by microfluidics-based capillary electrophoresis using an RNA 6000 Nano kit Bioanalyzer (Agilent Technologies). The sample labeling was performed using a Quick-Amp labeling kit, One Color (Agilent Technologies). Next, a cDNA master mix was added to the denatured RNA sample and incubated at 40°C for 2 h for double-stranded cDNA synthesis. For cRNA synthesis, newly synthesized double-stranded cDNA was used as the template, and *in vitro* transcription was performed for 2 h 30 min at 40°C to incorporate Cy3 CTP. The fragmentation of labeled cRNA and hybridization were carried out using the Gene Expression Hybridization kit (Agilent Technologies). The hybridized slides were washed with Gene Expression wash buffers (Agilent Technologies) and scanned using the Microarray Scanner (Agilent Technologies). Data extraction from images was performed using Feature Extraction software (version 11.5.1.1; Agilent Technologies). The extracted raw data were analyzed using GeneSpring GX software (Agilent Technologies). Normalization of the data was performed in GeneSpring GX using the 75th percentile shift method, and fold change values were obtained by comparing test samples with respect to specific control samples. Genes showing fold upregulation of $>$0.6 (log base 2) or fold downregulation <-0.6 (log base 2) in the test samples relative to that in the control sample were identified. *P* values of replicate data sets were calculated by Student's *t* test based on a volcano plot algorithm. Differentially regulated genes were clustered using hierarchical clustering based on a Pearson coefficient correlation algorithm to identify significant gene expression patterns. Genes were classified based on functional category and pathways using the biological analysis tool DAVID (http://david.abcc.ncifcrf.gov/).

Quantitative real-time RT-PCR. Total RNA was extracted from each bacterial culture grown with or without heat shock as described above. cDNA synthesis and PCRs were performed using a Superscript III platinum-SYBR green one-step qRT-PCR kit (Invitrogen) with appropriate primer pairs (200 nM). RT-qPCR cycling conditions in a real-time PCR detection system (Applied Biosystems) were as follows: 50°C for 45 min and 95°C for 5 min, each for one cycle followed by 40 cycles of 95°C for 15 s and 65°C for 30 s. To evaluate the PCR efficiency, a standard curve was generated for each pair of primers using serially diluted RNA samples, and PCR efficiency was always within the acceptable range of 95% to 105%. The endogenously expressed *M. tuberculosis gapdh* (Rv1436) was used to normalize each sample, and approximate fold difference was calculated using the $\Delta\Delta C_T$ method (31). The average fold changes in expression levels of genes and standard deviations from replicates of experiments were determined from at least three independent RNA preparations. The oligonucleotide primers used in RT-qPCR experiments are listed in Table S1. Control reactions with platinum *Taq* DNA polymerase (Invitrogen) confirmed the absence of genomic DNA in all our RNA preparations.

Cloning. Isolation and purification of nucleic acids, digestion with restriction enzymes, other enzymatic manipulations, and analyses of nucleic acids or fragments by agarose gel electrophoresis were according to standard procedures (11). An *M. tuberculosis hspR* overexpression construct has been described earlier (11). Likewise, truncated *hspR* (containing 348 bp of the open reading frame [ORF] excluding the terminal 30 bp), full-length *hrcA* (containing 1,029 bp of the ORF), and truncated *hrcA* (containing 975 bp of the ORF excluding the terminal 54 bp) were cloned in T7-lac-based expression system pET15b (Novagen) as recombinant fusion proteins containing an N-terminal His_6 tag. The cloning strategy resulted in pET-*hspR*Δ10, pET-*hrcA*, and pET-*hrcA*Δ18 comprising 116 amino acids of HspR lacking the C-terminal 10 residues of HspR, 343 amino acids of full-length HrcA, and 325 amino acids of HrcA lacking the C-terminal 18 residues of HrcA, respectively. GST-tagged PhoP and HspR have been described earlier (11, 32). Plasmid pGEX-*hrcA* expressing HrcA with an N-terminal GST tag was generated by cloning PCR-derived *hrcA* ORF fragment between BamHI and XhoI sites of pGEX 4T-1 (GE Healthcare).

To complement *hrcA* and *hspR* expression in the respective mycobacterial mutants, the ORFs were cloned and expressed in mycobacterial expression vector pSTKi (13). To express FLAG-tagged *hrcA* in *M. tuberculosis*, the ORFs were cloned and expressed in mycobacterial expression vector p19Kpro (14). The list of oligonucleotide primers used in cloning is provided in Table S2. In all cases, nucleotide sequences of the constructs were verified by automated DNA sequencing.

Construction of *M. tuberculosis* gene replacement mutants. The 5′ homology (1,030 bp encompassing bp −1000 to +30) and the 3′ homology (1,030 bp encompassing the distal 30 bases of the respective ORFs and 1,000 bases downstream) of Rv0353 and Rv2374c, respectively, were amplified from the *M. tuberculosis* H37Rv genomic DNA by KOD DNA polymerase (Toyobo Biosciences) using appropriate primer pairs (Table S2). The primers contained pflMI sites in the flanks to yield ends compatible for cloning with the *hyg* cassette (amplified using specific primers) and oriEp cosI fragment generated from p0004S (a kind gift of W. Jacob). Also, EcoRV sites were inserted both in the 5′ flank of the forward primer and the 3′ flank of the reverse primer. The amplicons comprising homologous sequences at both the 5′ and 3′ ends and *hyg* cassette were next digested with pflMI and ligated to the oriEp cosI fragment to generate the allelic exchange substrate (AES). Next, the AES was digested with EcoRV to generate linear AES for recombineering. To generate the mutants, *M. tuberculosis* H37Rv was electroporated with pNit-ET (a kind gift of E. Rubin [33]), the transformed cells were grown until an A_{600} of 0.4, the expression of recombineering proteins was induced by the addition of 5 μM isovaleronitrile, and the cultures were allowed to grow until an A_{600} of 0.8. Electrocompetent cells, prepared as described previously (12), were then electroporated with 200 ng of linear AES. Transformed colonies were selected on a 7H11 agar plate containing 100 μg/ml Hyg; a few colonies were picked up, cells were grown, and genomic DNA was isolated. Finally, the potential colonies were screened by PCR using specific primers to confirm the gene replacement mutants. The Δ*phoP*, Δ*sigE*, and Δ*sigH* mutants of *M. tuberculosis* and the correspondingly complemented strains have been described earlier (28, 34, 35). The following antibiotics were used as appropriate: hygromycin (Hyg), 100 μg/ml; kanamycin (Kan), 20 μg/ml. Studies related to *M. tuberculosis* H37Rv strains were carried out in a biosafety level 3 (BSL3) facility per institutional biosafety guidelines.

Southern blot hybridization. For Southern blot analyses, approximately 1 μg of genomic DNA of WT and mutant *M. tuberculosis* strains was digested with BamHI and resolved by agarose gel electrophoresis. The DNA samples were next transferred onto an Immobilon membrane (Millipore) by vacuum-based blotting and hybridized with radiolabeled gene-specific probes. The *hrcA*- and *hspR*-specific probes were generated by PCR using [α-^{32}P]dCTP (BRIT, India) and oligonucleotide primers (Table S2), which were used to clone the respective ORFs; prehybridization, hybridization, and washing steps were carried out as described previously (36). The results were developed and digitalized with a Fuji phosphorimager (GE Healthcare).

Proteins. *M. tuberculosis* PhoP and its domains were expressed and purified as described previously (21). Full-length and truncated HrcA and truncated HspR were expressed in *E. coli* BL21(DE3) as fusion proteins containing an N-terminal His_6 tag and purified by immobilized metal-affinity chromatography (Ni-NTA; Qiagen) as described previously for HspR (11). Both the full-length and the truncated variants of HspR and HrcA were expressed with N-terminal GST tags, as described for GST-PhoP (11). Finally, the proteins were stored in buffer containing 50 mM Tris-HCl (pH 7.9), 500 mM NaCl, and 10% glycerol. In all cases, the purity was verified by SDS-PAGE, protein concentrations were determined by Bradford reagent with bovine serum albumin (BSA) as the standard, and the results were compared with Quant-iT protein assay kits/Qubit fluorometer (Invitrogen) and expressed as equivalents of protein monomers.

Immunoblotting. Cell lysates of *M. tuberculosis* were resolved by 12% SDS-PAGE and visualized by Coomassie blue staining or by Western blot analysis. For immunoblotting, resolved samples were electroblotted onto polyvinylidene difluoride (PVDF) membranes (Millipore) and were detected by affinity-purified anti-PhoP, anti-HspR, and anti-HrcA antibodies elicited in rabbit (Bioneeds). RNA polymerase was used as a loading control and was detected with a monoclonal antibody against the β subunit of RNA polymerase, RpoB (Abcam). Anti-His and anti-GST antibodies were from GE Healthcare. Goat anti-rabbit and goat anti-mouse secondary antibodies (Abexome Biosciences) conjugated to horseradish peroxidase were used. Blots were developed with Luminata Forte chemiluminescence reagent (Millipore).

Chromatin IP. ChIP experiments using actively growing cultures of *M. tuberculosis* were performed as described previously (37). DNA-protein complexes in growing cells were crosslinked by 1% formaldehyde for 20 min, and cross-linking was quenched by the addition of 125 mM glycine. Immunoprecipitation (IP) was carried out using affinity-purified anti-PhoP (Alpha Omega Sciences) or anti-FLAG antibodies (Thermo Scientific) and protein A/G-agarose beads (Pierce). qPCR was performed using PAGE-purified primer pairs (Sigma) (Table S1) that contained appropriate promoter regions of interest. Typically, 40 cycles of amplifications were carried out in a real-time PCR detection system (Applied Biosystems) using serially diluted DNA samples (mock, IP treated, and total input). *In vivo* recruitment of PhoP or HrcA was examined by ChIP-qPCR using appropriate dilutions of IP DNA in a reaction buffer containing SYBR green mix (Invitrogen), 0.2 μM page-purified primers, and 1 U Platinum *Taq* DNA polymerase (Invitrogen). Enrichment of PCR signal from the anti-PhoP or anti-FLAG IP relative to the signal from an IP experiment without adding any antibody (mock) was measured to determine the efficiency of recruitment. The specificity of PCR enrichment was verified by performing ChIP-qPCR on identical IP samples using *gapdh*-specific primers. Data represent the means of duplicate qPCR measurements using at least three independent *M. tuberculosis* cultures. In all cases, melting curve analysis was carried out to confirm amplification of a single product.

Electrophoretic mobility shift assays. Purified proteins (HspR and its truncated variant) were used to assess DNA binding to the acr2up2 promoter fragment as described previously (11). The PCR-amplified

fragment was end labeled with [γ-^{32}P]ATP (1,000 Ci nmol^{-1}) using T4 polynucleotide kinase and purified from the free label by Sephadex G-50 spin columns (GE Healthcare). Next, various concentrations of purified proteins were incubated with the end-labeled probe in a total volume of 10 or 20 μl binding mix (50 mM Tris-HCl [pH 7.5], 50 mM NaCl, 0.2 mg/ml of bovine serum albumin, 10% glycerol, 1 mM dithiothreitol, ≈50 ng of labeled DNA probe, and 0.2 μg of sheared herring sperm DNA) at 20°C for 20 min. To resolve DNA-protein complexes, samples were analyzed by electrophoresis on a 6% (wt/vol) nondenaturing polyacrylamide gel in 0.5× TBE (89 mM Tris base, 89 mM boric acid, and 2 mM EDTA) at 70 V and 4°C. The position of the radioactive material was determined by exposure to a phosphor storage screen, and bands were quantified by the phosphorimager (Fuji).

Mycobaterial protein fragment complementation assays. To express *M. tuberculosis* PhoP or its domains in *M. smegmatis*, the *phoP* gene and its domain constructs were cloned in the integrative vector pUAB400 (Kan^r) (Table 1) between MfeI and HindIII sites, as described previously (11). Similarly, *hrcA*, truncated *hrcA*, and truncated *hspR* were cloned in episomal plasmid pUAB300 (Hyg^r) (Table 1) between BamHI/HindIII sites to generate pUAB300-*hrcA*, pUAB300-*hrcA*Δ18, and pUAB300-*hspR*Δ10, respectively, as described for pUAB300-*hspR* (11). The constructs were verified by DNA sequencing. Next, cotransformed cells were selected on 7H10-Kan-Hyg plates, and M-PFC experiments were performed as described previously (11). As a positive control, ESAT-6/CFP-10 expressing constructs used in M-PFC experiments have been reported earlier (24).

Data availability. The data reported here, including a complete list of genes, have been deposited in the NCBI's Gene Expression Omnibus and are accessible through GEO series accession number GSE100596.

SUPPLEMENTAL MATERIAL

Supplemental material for this article may be found at https://doi.org/10.1128/JB.00013-19.

SUPPLEMENTAL FILE 1, PDF file, 0.7 MB.

ACKNOWLEDGMENTS

This work was supported by, a research grant (to D.S.) from SERB (EMR/2016/004904), Department of Science and Technology (DST), and by intramural support from the Council of Scientific and Industrial Research (CSIR), Government of India. R.R.S. and R.S. were supported by CSIR; D.A. and P.R.S. were supported by SERB, DST and DBT, respectively, for their predoctoral fellowships.

The funders had no role in the study design, data collection and interpretation, or the decision to submit the work for publication.

We thank Arthur Landy for critical reading of the manuscript. We also thank G. Marcela Rodriguez and Issar Smith (The Public Health Research Institute, New Jersey Medical School, UMDNJ) for Δ*phoP* and the complemented *M. tuberculosis* strains, Eric Rubin (Harvard School of Public Health) for the pNIT plasmid, Adrie Steyn (University of Alabama) and Ashwani Kumar (CSIR-IMTECH) for pUAB300/pUAB400 plasmids, and Hayden T. Pacl (Steyn Lab, University of Alabama) for generating the heat map from the microarray data. We thank Roohi Bansal for preliminary M-PFC results, V. Anil Kumar for helpful discussions, and Renu Sharma for technical assistance. We acknowledge Genotypic Technology Private Limited (India) for the microarray results and data analysis reported in this work.

We declare no conflict of interest.

R.R.S., D.A., P.R.S., R.S., V.K.N., S.K., and D.S. designed the research; R.R.S., D.A., P.R.S., R.S., and S.K. performed the research; D.A., V.K.N., and S.K. contributed new reagents; R.R.S., R.S., S.K., and D.S. analyzed the data; D.S. conceived and coordinated the study and wrote the paper; R.R.S., V.K.N., and S.K contributed to writing the final version of the manuscript.

REFERENCES

1. Monahan IM, Betts J, Banerjee DK, Butcher PD. 2001. Differential expression of mycobacterial proteins following phagocytosis by macrophages. Microbiology 147:459–471. https://doi.org/10.1099/00221287-147-2-459.
2. Schnappinger D, Ehrt S, Voskuil MI, Liu Y, Mangan JA, Monahan IM, Dolganov G, Efron B, Butcher PD, Nathan C, Schoolnik GK. 2003. Transcriptional adaptation of *Mycobacterium tuberculosis* within macrophages: insights into the phagosomal environment. J Exp Med 198:693–704. https://doi.org/10.1084/jem.20030846.
3. Asea A, Kabingu E, Stevenson MA, Calderwood SK. 2000. HSP70 peptide-bearing and peptide-negative preparations act as chaperokines. Cell Stress Chaperones 5:425–431. https://doi.org/10.1379/1466-1268(2000)005<0425:HPBAPN>2.0.CO;2.
4. Stewart GR, Wernisch L, Stabler R, Mangan JA, Hinds J, Laing KG, Young DB, Butcher PD. 2002. Dissection of the heat-shock response in *Mycobacterium tuberculosis* using mutants and microarrays. Microbiology 148:3129–3138. https://doi.org/10.1099/00221287-148-10-3129.

5. Lee BY, Horwitz MA. 1995. Identification of macrophage and stress-induced proteins of *Mycobacterium tuberculosis*. J Clin Invest 96:245–249. https://doi.org/10.1172/JCI118028.
6. Stewart GR, Snewin VA, Walzl G, Hussell T, Tormay P, O'Gaora P, Goyal M, Betts J, Brown IN, Young DB. 2001. Overexpression of heat-shock proteins reduces survival of *Mycobacterium tuberculosis* in the chronic phase of infection. Nat Med 7:732–737. https://doi.org/10.1038/89113.
7. Stewart GR, Newton SM, Wilkinson KA, Humphreys IR, Murphy HN, Robertson BD, Wilkinson RJ, Young DB. 2005. The stress-responsive chaperone alpha-crystallin 2 is required for pathogenesis of *Mycobacterium tuberculosis*. Mol Microbiol 55:1127–1137. https://doi.org/10.1111/j.1365-2958.2004.04450.x.
8. Raman S, Song T, Puyang X, Bardarov S, Jacobs WR, Jr, Husson RN. 2001. The alternative sigma factor SigH regulates major components of oxidative and heat stress responses in *Mycobacterium tuberculosis*. J Bacteriol 183:6119–6125. https://doi.org/10.1128/JB.183.20.6119-6125.2001.
9. Frigui W, Bottai D, Majlessi L, Monot M, Josselin E, Brodin P, Garnier T, Gicquel B, Martin C, Leclerc C, Cole ST, Brosch R. 2008. Control of *M. tuberculosis* ESAT-6 secretion and specific T cell recognition by PhoP. PLoS Pathog 4:e33. https://doi.org/10.1371/journal.ppat.0040033.
10. Lee JS, Krause R, Schreiber J, Mollenkopf HJ, Kowall J, Stein R, Jeon BY, Kwak JY, Song MK, Patron JP, Jorg S, Roh K, Cho SN, Kaufmann SH. 2008. Mutation in the transcriptional regulator PhoP contributes to avirulence of *Mycobacterium tuberculosis* H37Ra strain. Cell Host Microbe 3:97–103. https://doi.org/10.1016/j.chom.2008.01.002.
11. Singh R, Anil Kumar V, Das AK, Bansal R, Sarkar D. 2014. A transcriptional co-repressor regulatory circuit controlling the heat-shock response of *Mycobacterium tuberculosis*. Mol Microbiol 94:450–465. https://doi.org/10.1111/mmi.12778.
12. van Kessel JC, Hatfull GF. 2007. Recombineering in *Mycobacterium tuberculosis*. Nat Methods 4:147–152. https://doi.org/10.1038/nmeth996.
13. Parikh A, Kumar D, Chawla Y, Kurthkoti K, Khan S, Varshney U, Nandicoori VK. 2013. Development of a new generation of vectors for gene expression, gene replacement, and protein-protein interaction studies in mycobacteria. Appl Environ Microbiol 79:1718–1729. https://doi.org/10.1128/AEM.03695-12.
14. De Smet KA, Kempsell KE, Gallagher A, Duncan K, Young DB. 1999. Alteration of a single amino acid residue reverses fosfomycin resistance of recombinant MurA from *Mycobacterium tuberculosis*. Microbiology 145:3177–3184. https://doi.org/10.1099/00221287-145-11-3177.
15. Anil Kumar V, Goyal R, Bansal R, Singh N, Sevalkar RR, Kumar A, Sarkar D. 2016. EspR-dependent ESAT-6 protein secretion of *Mycobacterium tuberculosis* requires the presence of virulence regulator PhoP. J Biol Chem 291:19018–19030. https://doi.org/10.1074/jbc.M116.746289.
16. Singh A, Mai D, Kumar A, Steyn AJ. 2006. Dissecting virulence pathways of *Mycobacterium tuberculosis* through protein-protein association. Proc Natl Acad Sci U S A 103:11346–11351. https://doi.org/10.1073/pnas.0602817103.
17. Kelley LA, Mezulis S, Yates CM, Wass MN, Sternberg MJ. 2015. The Phyre2 web portal for protein modeling, prediction and analysis. Nat Protoc 10:845–858. https://doi.org/10.1038/nprot.2015.053.
18. Newberry KJ, Huffman JL, Miller MC, Vazquez-Laslop N, Neyfakh AA, Brennan RG. 2008. Structures of BmrR-drug complexes reveal a rigid multidrug binding pocket and transcription activation through tyrosine expulsion. J Biol Chem 283:26795–26804. https://doi.org/10.1074/jbc.M804191200.
19. Liu J, Huang C, Shin DH, Yokota H, Jancarik J, Kim JS, Adams PD, Kim R, Kim SH. 2005. Crystal structure of a heat-inducible transcriptional repressor HrcA from *Thermotoga maritima*: structural insight into DNA binding and dimerization. J Mol Biol 350:987–996. https://doi.org/10.1016/j.jmb.2005.04.021.
20. Pierce BG, Wiehe K, Hwang H, Kim BH, Vreven T, Weng Z. 2014. ZDOCK server: interactive docking prediction of protein-protein complexes and symmetric multimers. Bioinformatics 30:1771–1773. https://doi.org/10.1093/bioinformatics/btu097.
21. Pathak A, Goyal R, Sinha A, Sarkar D. 2010. Domain structure of virulence-associated response regulator PhoP of *Mycobacterium tuberculosis*: role of the linker region in regulator-promoter interaction(s). J Biol Chem 285:34309–34318. https://doi.org/10.1074/jbc.M110.135822.
22. Bandyopadhyay B, Das Gupta T, Roy D, Das Gupta SK. 2012. DnaK dependence of the mycobacterial stress-responsive regulator HspR is mediated through its hydrophobic C-terminal tail. J Bacteriol 194:4688–4697. https://doi.org/10.1128/JB.00415-12.
23. He X, Wang L, Wang S. 2016. Structural basis of DNA sequence recognition by the response regulator PhoP in *Mycobacterium tuberculosis*. Sci Rep 6:24442. https://doi.org/10.1038/srep24442.
24. Bansal R, Anil Kumar V, Sevalkar RR, Singh PR, Sarkar D. 2017. *Mycobacterium tuberculosis* virulence-regulator PhoP interacts with alternative sigma factor SigE during acid-stress response. Mol Microbiol 104:400–411. https://doi.org/10.1111/mmi.13635.
25. Hobman JL. 2007. MerR family transcription activators: similar designs, different specificities. Mol Microbiol 63:1275–1278. https://doi.org/10.1111/j.1365-2958.2007.05608.x.
26. Brown NL, Stoyanov JV, Kidd SP, Hobman JL. 2003. The MerR family of transcriptional regulators. FEMS Microbiol Rev 27:145–163. https://doi.org/10.1016/S0168-6445(03)00051-2.
27. Stapleton MR, Smith LJ, Hunt DM, Buxton RS, Green J. 2012. *Mycobacterium tuberculosis* WhiB1 represses transcription of the essential chaperonin GroEL2. Tuberculosis (Edinb) 92:328–332. https://doi.org/10.1016/j.tube.2012.03.001.
28. Walters SB, Dubnau E, Kolesnikova I, Laval F, Daffe M, Smith I. 2006. The *Mycobacterium tuberculosis* PhoPR two-component system regulates genes essential for virulence and complex lipid biosynthesis. Mol Microbiol 60:312–330. https://doi.org/10.1111/j.1365-2958.2006.05102.x.
29. Goyal R, Das AK, Singh R, Singh PK, Korpole S, Sarkar D. 2011. Phosphorylation of PhoP protein plays direct regulatory role in lipid biosynthesis of *Mycobacterium tuberculosis*. J Biol Chem 286:45197–45208. https://doi.org/10.1074/jbc.M111.307447.
30. Amin-Ul Mannan M, Sharma S, Ganesan K. 2009. Total RNA isolation from recalcitrant yeast cells. Anal Biochem 389:77–79. https://doi.org/10.1016/j.ab.2009.03.014.
31. Schmittgen TD, Livak KJ. 2008. Analyzing real-time PCR data by the comparative C(T) method. Nat Protoc 3:1101–1108. https://doi.org/10.1038/nprot.2008.73.
32. Gupta S, Pathak A, Sinha A, Sarkar D. 2009. *Mycobacterium tuberculosis* PhoP recognizes two adjacent direct-repeat sequences to form head-to-head dimers. J Bacteriol 191:7466–7476. https://doi.org/10.1128/JB.00669-09.
33. Wei JR, Krishnamoorthy V, Murphy K, Kim JH, Schnappinger D, Alber T, Sassetti CM, Rhee KY, Rubin EJ. 2011. Depletion of antibiotic targets has widely varying effects on growth. Proc Natl Acad Sci U S A 108:4176–4181. https://doi.org/10.1073/pnas.1018301108.
34. Manganelli R, Voskuil MI, Schoolnik GK, Smith I. 2001. The *Mycobacterium tuberculosis* ECF sigma factor sigmaE: role in global gene expression and survival in macrophages. Mol Microbiol 41:423–437. https://doi.org/10.1046/j.1365-2958.2001.02525.x.
35. Manganelli R, Voskuil MI, Schoolnik GK, Dubnau E, Gomez M, Smith I. 2002. Role of the extracytoplasmic-function sigma factor sigma(H) in *Mycobacterium tuberculosis* global gene expression. Mol Microbiol 45:365–374. https://doi.org/10.1046/j.1365-2958.2002.03005.x.
36. Sambrook J, Fritsch EF, Maniatis T. 1989. Molecular cloning: a laboratory manual, 2nd ed. Cold Spring Harbor Laboratory Press, Cold Spring Harbor, N.Y.
37. Fol M, Chauhan A, Nair NK, Maloney E, Moomey M, Jagannath C, Madiraju MV, Rajagopalan M. 2006. Modulation of *Mycobacterium tuberculosis* proliferation by MtrA, an essential two-component response regulator. Mol Microbiol 60:643–657. https://doi.org/10.1111/j.1365-2958.2006.05137.x.
38. Edgar R, Domrachev M, Lash AE. 2002. Gene Expression Omnibus: NCBI gene expression and hybridization array data repository. Nucleic Acids Res 30:207–210. https://doi.org/10.1093/nar/30.1.207.